Inorganic Chemistry

Article

pubs.acs.org/IC

Homochiral 1D Helical Chain Based on an Achiral Cu(II) Complex

Chihiro Kachi-Terajima,*[,†,‡] Megumi Ishii,[†] Toshiaki Saito,[‡,§] Chikahide Kanadani,[‡] Takunori Harada,[∥,⊥] and Reiko Kuroda[∥,#]

[†]Department of Chemistry, Faculty of Science, Toho University, 2-2-1 Miyama, Funabashi, Chiba 274-8510, Japan

[‡]Research Center for Materials with Integrated Properties, Toho University, 2-2-1 Miyama, Funabashi, Chiba 274-8510, Japan

[§]Department of Physics, Faculty of Science, Toho University, 2-2-1 Miyama, Funabashi, Chiba 274-8510, Japan

[∥]ERATO-SORST Kuroda Chiromorphology Team, Japan Science and Technology Agency; Department of Life Sciences, Graduate School of Arts and Sciences, The University of Tokyo, 3-8-1 Komaba, Meguro-ku, Tokyo 153-8902, Japan

Supporting Information

ABSTRACT: Self-assembly of an achiral [Cu(L)] complex produced a homochiral helical chain $[Cu(L)]_3 \cdot 2H_2O$ (**1**) (L = 2-dimethylaminoethyl(oxamato)). Interestingly, complex **1** obtained in our laboratory exhibits only a left-handed helical chain without any chiral source. Single-crystal X-ray analysis revealed the absolute structure and homochirality of its helical chain structure in the space group of $P3_2$. Solid-state circular dichroism (CD) spectra confirmed the high enantio excess of the crystals obtained in different synthesis batches. Magnetic susceptibility measurements reveal a relatively strong intrachain antiferromagnetic interaction between Cu(II) centers via an oxamato bridge ($J = -74.4$ cm^{-1}).

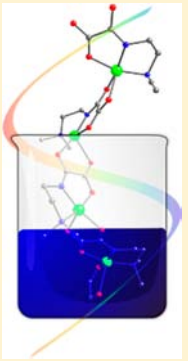

INTRODUCTION

Chiral symmetry breaking is known to occur in the biosphere. The large excess of one enantiomer in nature, e.g., L-amino acids and D-sugars, is an intriguing phenomenon.[1] Such phenomenon can be also observed in the chiral crystallization of achiral molecules in the organic or inorganic systems as well as chiral molecules. While two enantiomers are generally produced with equal probability in the absence of any chiral source, it is known that spontaneous chiral symmetry breaking can occur in the stirred crystallization of achiral $NaClO_3$.[2] Examples of chiral crystallization are also known in achiral organic compounds.[3] In the case of metal complexes, chirality can be induced by chiral assembly through coordination of ligand or complex units, even though they are achiral.[4] Herein we report a left-handed helical chain (space group $P3_2$), [Cu(L)]*n*, obtained by self-assembly of the achiral [Cu(L)] complex that can act as a ligand, a so-called metalloligand. Little is known about the chiral crystallization by self-aggregation based on coordination of the achiral complex. Crystallographic data of the right-handed helical chain of this complex (the enantiomorph $P3_1$) has been reported in a private communication from Parsons et al.[5] However, only the left-handed spiral of the Cu chain has been obtained in our laboratory without any chiral source. We found the homochirality of our crystals by solid-state CD spectra and X-ray crystallography. The synthesis, structures, and characterization for **1** are described.

EXPERIMENTAL SECTION

Materials. All chemicals used in the syntheses were of regent grade and used without further purification.

Preparation of Ligand Precursor: Methyl 2-(dimethylaminoethylamino)-2-oxoacetate. Methyl chloroglyoxylate (4.150 g, 33.9 mmol) in THF (100 mL) was added dropwise to a THF solution (200 mL) of *N*,*N*-dimethylethylenediamine (3.000 g, 34.0 mmol) at room temperature, and the reaction mixture was stirred at the same temperature for 30 min. The white precipitate was formed and collected by filtration. It was washed with THF and dried. Yield: 5.110 g, 86.6%. IR (cm^{-1}) (KBr): 3544, 1742, 1697, 1222. ^{1}H NMR (400 MHz, D_2O): 2.97 (s, 6H), 3.41 (t, 2H), 3.75 (t, 2H), 3.93 (s, 3H).

Preparation of $[Cu(L)]_3 \cdot 2H_2O$ (1). The ligand precursor (0.348 g, 2.00 mmol) and KOH (0.375 g, 6.68 mmol) were dissolved in 3.0 mL of water, and then the mixture was stirred for 30 min at 60 °C. The aqueous solution (2.0 mL) of $CuSO_4$ (0.290 g, 1.82 mmol) was added; the mixture was stirred at 60 °C to reduce the volume to 3.5 mL. The resulting solution was filtered, and the filtrate was slowly evaporated to give complex **1** as deep-blue crystals. Yield: 0.165 g, 41.0%. Anal. Calcd for $C_{18}H_{34}Cu_3N_6O_{11}$: C, 30.83; H, 4.89; N, 11.99. Found: C, 30.85; H, 4.64; N, 11.98. IR (cm^{-1}) (KBr): 1682, 1615, 1335, 1309, 803.

Physical Measurements. Infrared spectra were measured on KBr disks with a JASCO FT-IR-4100. Elemental analyses for CHN were performed using a CHN-corder (Yanako MT-6). The amount of crystalline solvents in the crystals was determined by thermogravimetric (TG) analyses (SII EXSTAR 6000 (TG-DTA 6200) system) under a nitrogen atmosphere at a heating rate of 5 °C/min. The CD spectrum of the solution was recorded on a JASCO J-820

Received: December 15, 2011
Published: June 28, 2012

Table 1. Crystal Data and Structure Refinements for 1

compound	**1**
empirical formula	$C_{18}H_{34}Cu_3N_6O_{11}$
M/g mol^{-1}	701.13
T/K	100(2)
cryst syst	trigonal
space group	$P3_2$
a/Å	12.7814(6)
b/Å	12.7814(6)
c/Å	13.5912(12)
α/deg	90
β/deg	90
γ/deg	120
V/Å^3	1922.8(2)
Z	3
D_{calcd}/g cm^{-3}	1.816
reflns collected	14 316
indep reflns (R_{int})	5848 (0.0180)
goodness of fit	1.061
$R1$ ($I > 2\sigma$ (all data))[a]	0.0241 (0.0252)
w$R2$ ($I > \sigma 2$ (all data))[b]	0.0640 (0.0643)
least diff. peak (hole)/e Å^{-3}	0.526 (−0.613)
Flack param	0.014(8)

[a] $R1 = \Sigma||F_o| - |F_c||/\Sigma|F_o|$. [b] $wR2 = \{\Sigma[\ w(F_o^2 - F_c^2)^2\ ]/\Sigma[w(F_o^2)^2]\}^{1/2}$.

spectrophotometer. Solid-state CD spectra were measured on KBr disks with a solid-state dedicated universal chiroptical spectrophotometer (UCS-1: JASCO J-800KCM).[6]

Structure Determinations. A single crystal of **1** was mounted on a glass fiber in inert oil to avoid a reduction of crystalline solvent molecules. Data collection was performed on a Bruker SMART APEX area detector diffractometer with a graphite monochromator and Mo Kα radiation, λ = 0.71073 Å. Empirical adsorption correction was applied using the SADABS program. Structures were solved by direct methods (SHELXS 97) and refined by full-matrix least-squares calculations on F^2 (SHELXL-97) with the SHELX-TL program package. All of the non-hydrogen atoms were refined anisotropically. Hydrogen atoms of the core structure were fixed at calculated positions and refined with a riding model. Hydrogen atoms of some water molecules cannot be located because of their disordered nature. Crystallographic data and selected bond distances/angles are summarized in Tables 1 and 2, respectively. CCDC-XXXXXXXXXXX for **1** contains the supplementary crystallographic data. This data can be obtained free of charge from the Cambridge Crystallographic Data Centre via http://www.ccdc.cam.ac.uk/data_request/cif.

RESULTS AND DISCUSSION

Complex [Cu(L)] was prepared by reaction of ligand precursor methyl 2-(dimethylaminoethylamino)-2-oxoacetate with

Scheme 1. (a) Synthesis of Complex 1. (b) Formation of a Left-Handed Helical Chain by Self-Assembly

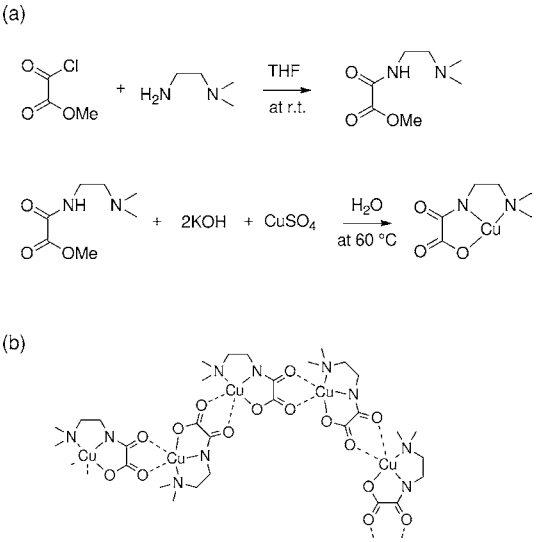

Table 2. Selected Bond Distances (Angstroms) and angles (degrees) with Estimated Standard Deviations in Parentheses for 1[a]

Cu(1)−O(1)	2.001(1)	intrachain		N(1)−Cu(1)−N(2)	82.68(9)	N(3)−Cu(2)−N(4)	83.64(9)	N(5)−Cu(3)−N(6)	83.43(10)
Cu(1)−N(1)	1.909(2)	Cu(1)···Cu(1)$^{\#1}$	5.3081(6)	N(1)−Cu(1)−O(1)	83.20(8)	N(3)−Cu(2)−O(4)	82.55(8)	N(5)−Cu(3)−O(7)	83.12(9)
Cu(1)−N(2)	2.056(2)	Cu(2)···Cu(2)$^{\#2}$	5.3347(5)	N(1)−Cu(1)−O(2)$^{\#1}$	98.71(8)	N(3)−Cu(2)−O(5)$^{\#2}$	112.65(8)	N(5)−Cu(3)−O(8)$^{\#3}$	110.00(9)
Cu(1)−O(2)$^{\#1}$	2.265(1)	Cu(3)···Cu(3)$^{\#3}$	5.2882(6)	N(1)−Cu(1)−O(3)$^{\#1}$	177.56(9)	N(3)−Cu(2)−O(6)$^{\#2}$	166.64(8)	N(5)−Cu(3)−O(9)$^{\#3}$	169.07(9)
Cu(1)−O(3)$^{\#1}$	1.940(1)	interchain		N(2)−Cu(1)−O(2)$^{\#1}$	96.49(8)	N(4)−Cu(2)−O(5)$^{\#2}$	99.41(8)	N(6)−Cu(3)−O(8)$^{\#3}$	98.28(9)
Cu(2)−O(4)	2.011(1)	Cu(1)···Cu(2)$^{\#2}$	6.3143(5)	O(1)−Cu(1)−N(2)	160.88(8)	O(4)−Cu(2)−N(4)	162.37(8)	O(7)−Cu(3)−N(6)	161.95(9)
Cu(2)−N(3)	1.922(2)	Cu(1)···Cu(3)	6.3133(5)	O(1)−Cu(1)−O(2)$^{\#1}$	98.33(8)	O(4)−Cu(2)−O(5)$^{\#2}$	96.00(7)	O(7)−Cu(3)−O(8)$^{\#3}$	97.60(8)
Cu(2)−N(4)	2.058(2)	Cu(2)···Cu(3)	6.4357(6)	O(3)$^{\#1}$−Cu(1)−N(2)	99.73(8)	O(6)$^{\#2}$−Cu(2)−N(4)	100.36(8)	O(9)$^{\#3}$−Cu(3)−N(6)	99.19(10)
Cu(2)−O(5)$^{\#2}$	2.284(1)			O(3)$^{\#1}$−Cu(1)−O(1)	94.54(7)	O(6)$^{\#2}$−Cu(2)−O(4)	90.81(7)	O(9)$^{\#3}$−Cu(3)−O(7)	91.91(8)
Cu(2)−O(6)$^{\#2}$	1.974(1)			O(3)$^{\#1}$−Cu(1)−O(2)$^{\#1}$	80.67(7)	O(6)$^{\#2}$−Cu(2)−O(5)$^{\#2}$	79.48(7)	O(9)$^{\#3}$−Cu(3)−O(8)$^{\#3}$	80.24(7)
Cu(3)−O(7)	2.006(1)								
Cu(3)−N(5)	1.910(2)								
Cu(3)−N(6)	2.043(3)								
Cu(3)−O(8)$^{\#3}$	2.274(1)								
Cu(3)−O(9)$^{\#3}$	1.956(1)								

[a] Symmetry operations: #1 ($-y$, $x - y$, $-1/3 + z$), #2 ($-x + y$, $1 - x$, $1/3 + z$), #3 ($1 - y$, $x - y$, $-1/3 + z$).

dx.doi.org/10.1021/ic202708e | Inorg. Chem. 2012, 51, 7502−7507

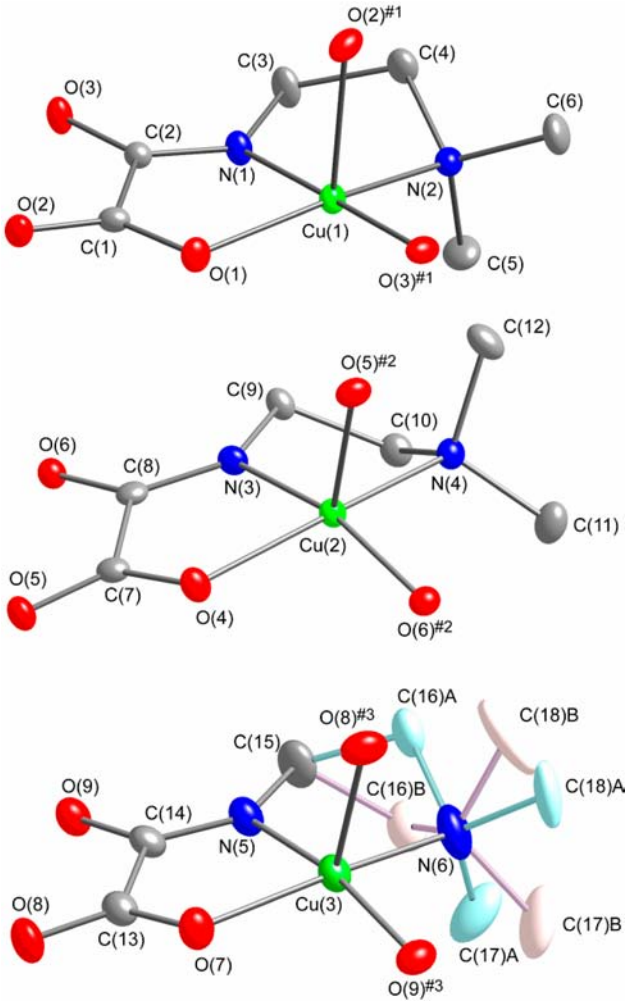

Figure 1. ORTEP drawings of crystallographically independent Cu(1), Cu(2), and Cu(3) molecules with thermal ellipsoids set at 50% probability, where hydrogen atoms and crystalline water molecules are omitted for clarity. Positional disorder of the dimethylaminoethyl group is found in the Cu(3) complex. Symmetry operations: #1 ($-y$, $x - y$, $-1/3 + z$), #2 ($-x + y$, $1 - x$, $1/3 + z$), #3 ($1 - y$, $x - y$, $-1/3 + z$).

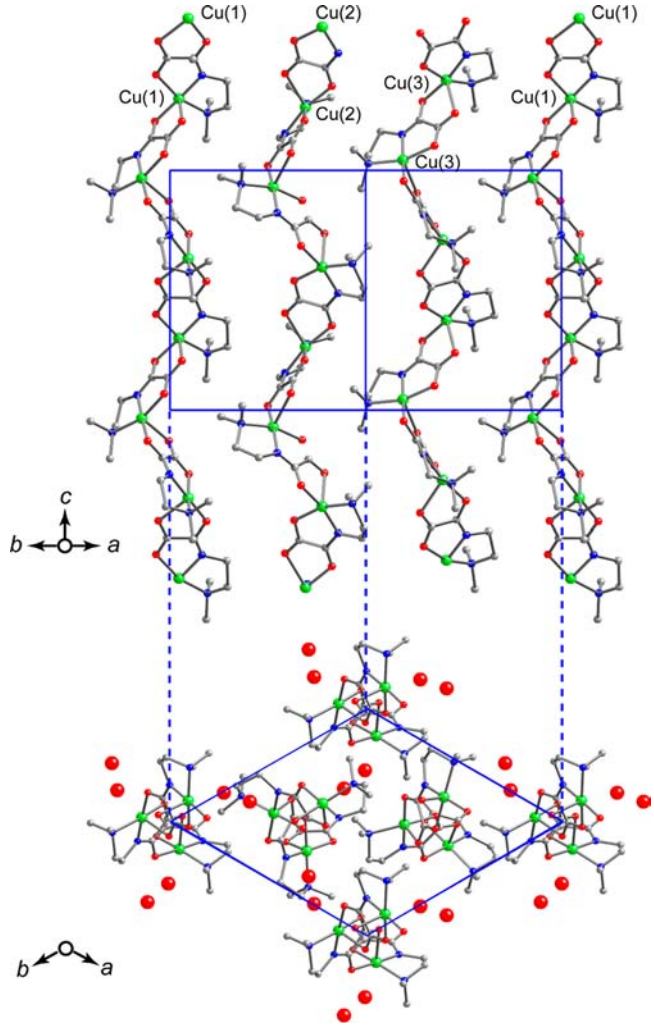

Figure 2. Packing diagrams of **1** showing the projection along the *ab* direction (top) and *c* axis (bottom). Interstitial water molecules located between chains are omitted for clarity in the top view and depicted in red ball in the bottom view.

$CuSO_4$ and KOH. Slow evaporation of the reaction mixture induced self-assembly of [Cu(L)] and yielded blue block crystals of **1** (Scheme 1 a). Complex **1** is structurally characterized by single-crystal X-ray analysis. Complex **1** crystallizes in the chiral trigonal $P3_2$ space group and adopts a left-handed helix (Scheme 1b). The absolute structure in the $P3_2$ space group was determined by a Flack parameter[7] of 0.014(8) using the least-squares method. The ORTEP drawing of **1** is depicted in Figure 1. There are three crystallographically independent Cu complexes in the asymmetric unit. These Cu(1), Cu(2), and Cu(3) complexes have very similar molecular structures. The molecular structure of Cu(1) complex therefore is described in detail as a representative example. The oxamato ligand is tridentate and occupies the equatorial position of the Cu(II) ion. The Cu(II) ion is 5 coordinate, with two nitrogen atoms and one oxygen atom from the equatorial ligand and two oxygen atoms from the neighboring oxamato moiety. The equatorial coordination sites are occupied by the set of N(1), N(2), O(1), $O(3)^{\#1}$ atoms (the average bond distances in the equatorial site are Cu–N = 1.983 Å and Cu–O = 1.971 Å). The bond distance for the axial coordinate, $Cu(1)–O(2)^{\#1}$ = 2.265(1) Å, is significantly longer than the equatorial ones, whose distortion is due to Jahn–Teller effects in the d^9 Cu(II) ion. Disorder of the dimethylaminoethyl group of the ligand was found only in Cu(3) complex. Although the ligand and the complex itself are achiral, each complex forms a left-handed helix by self-assembly through an oxamato bridge in the crystal. Actually, it is well known that the metal complexes can exhibit chirality on their supramolecular structures by self-assembly of metal ions and bridging ligand.[4] As shown in Figure 2, all three chains exhibit a left-handed helical conformation and chains of Cu(1) and Cu(3) are parallel to each other, while that of Cu(2) is antiparallel to them. The intrachain Cu···Cu distances through the oxamato bridge are 5.3081(6), 5.3347(5), and 5.2882(6) Å for the Cu(1), Cu(2), and Cu(3) chain, respectively. The nearest interchain Cu···Cu distances are 6.3143(5) Å for $Cu(1)···Cu(2)^{\#2}$, 6.3133(5) Å for Cu(1)···Cu(3), and 6.4357(6) Å for Cu(2)···Cu(3). The interstitial water molecules are located in the void space between the chains. The Cu(1) chain is linked to the Cu(2) and Cu(3) chains by the hydrogen bond between the oxygen atom of the ligand and interstitial water molecules (Figure 3). The O···O hydrogen bond

dx.doi.org/10.1021/ic202708e | *Inorg. Chem.* 2012, 51, 7502–7507

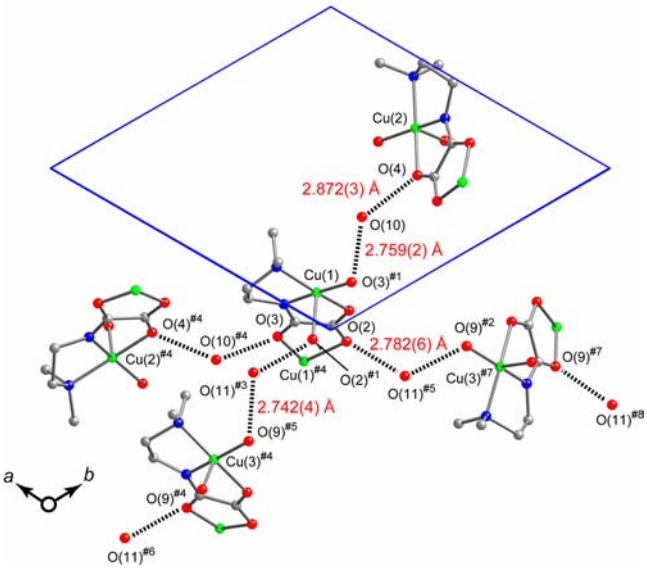

Figure 3. Crystal structure of **1**, showing a network structure connected by hydrogen bonds through crystalline water. Symmetry operations: #1 (−*y*, *x* − *y*, −1/3 + *z*), #2 (−*x* + *y*, 1 − *x*, 1/3 + *z*), #3 (1 − *y*, *x* − *y*, −1/3 + *z*), #4 (−*x* + *y*, −*x*, 1/3 + *z*), #5 (−1 + *x*, −1 + *y*, *z*), #6 (−1 + *x*, −2 + *y*, *z*), #7 (−*y*, *x* − *y*, 2/3 + *z*), #8 (−1 − x + *y*, 1 − *x*, 1/3 + *z*).

distances are in the range of 2.742(4)−2.872(3) Å. No intra- and interchain $\pi-\pi$ stacking were observed between CuL cores. The molecular structure (including bond distances and angles and the positional disorder of the dimethylaminoethyl group) and the packing feature are almost the same as those of the enantiomorph with $P3_1$ space group.

In the absence of any chiral source, we can obtain both $P3_1$ and $P3_2$ crystals with equal probability. However, the crystals obtained in different synthesis batches in our laboratory showed $P3_2$ space group, which were checked by single-crystal X-ray analysis. The $P3_2$ space group was observed in 9 single crystals obtained from 7 different preparations. In order to check the possibility of homochirality of **1**, we measured the solid-state CD spectra of the single crystal (165 μg) and polycrystals (167 μg) from 3 different batch preparations using a KBr pellet (Figure 4a and 4b). No structural change induced by grinding or dehydration of the interstitial water was observed in the XRD patterns (Figure S1, Supporting Information). The UV spectrum of aqueous solution of **1** is depicted in Figure 4c. Complex **1** became CD silent in the saturated aqueous solution because of its intrinsic achiral structure (Figure S2, Supporting Information). The crystals of **1** exhibit a negative Cotton effect centered at ca. 290 and ca. 660 nm and a positive one at 547 nm. A negative Cotton effect at around 660 nm corresponds to the d−d transition, which would reflect the chirality of the coordination sphere at the Cu(II) center. The curve of circular anisotropy factor, *g* (*g* = ΔOD/OD), was illustrated in Figure 4a and 4b. The maximum of the *g* factor at around 638 nm is −0.0029 for polycrystalline sample and −0.0037 for single-crystal sample, respectively. Although the *g* factor of polycrystals is slightly smaller than that of the single crystal, the data indicates the large excess of $P3_2$ crystals obtained in our laboratory. Unfortunately, it is unclear why a single chirality was generated in the different experimental condition (e.g., stirring and vessels for preparation) without chiral sources (e.g., seeding crystals and impurities). Such a phenomenon is rare

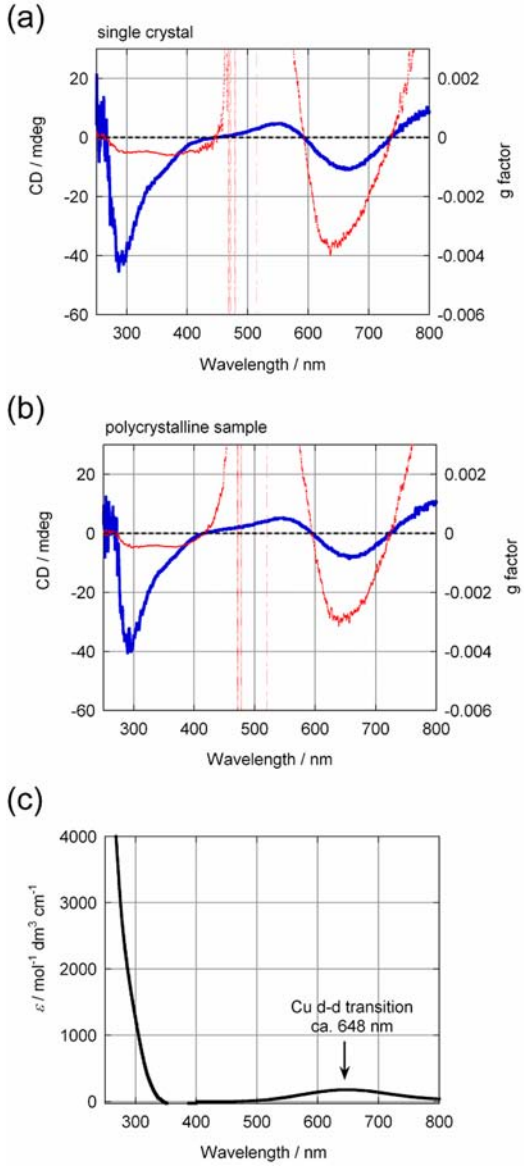

Figure 4. Solid-state CD spectra and *g* factor of (a) a single crystal and (b) polycrystals of **1**: CD, blue lines; *g* factor (*g* = ΔOD/OD), red line. (c) UV spectrum of **1** in aqueous solution.

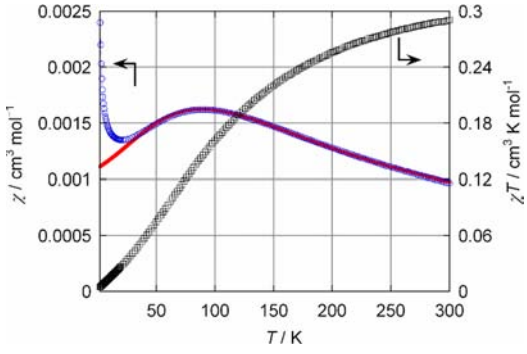

Figure 5. Temperature dependence of χ and χT measured on a polycrystalline sample of **1** at 1 kOe. Solid line corresponds to the best fits obtained with a Bonner−Fisher model for a spin 1/2 one-dimensional Heisenberg antiferromagnetic chains and the mean field approximation between 30 and 300 K.

dx.doi.org/10.1021/ic202708e | *Inorg. Chem.* 2012, 51, 7502−7507

but not surprising since chiral symmetry breaking is known to occur occasionally. However, this is a particularly intriguing example of chiral crystallization based on self-assembly of metal complexes.

Magnetic Properties of 1. The magnetic susceptibility of a polycrystalline sample of **1** was measured from 2.0 to 300 K applying a magnetic field of 1 kOe (Figure 5). The χT value continuously decreases upon cooling and reaches the minimum at 2.0 K. The susceptibilities obey the Curie–Weiss law above 205 K with C = 0.395 cm^3 K mol^{-1}, θ = −107 K (Figure S3, Supporting Information). The Curie constant is in agreement with the spin-only value of 0.376 cm^3 K mol^{-1} calculated by assuming g (Landé g factor) = 2.0 for one magnetically isolated Cu(II) ion (S = 1/2). The negative Weiss constant indicates the presence of antiferromagnetic interactions between Cu(II) centers. As shown in Figure 5, the susceptibility exhibits a maximum at 90 K followed by a minimum at 20 K. Below 20 K, the susceptibility curve rapidly increases with decreasing temperature, which is probably due to the presence of paramagnetic impurity or chain breaks induced by the defects. The temperature dependence of the magnetic susceptibility was fitted using a Bonner–Fisher antiferromagnetic S = 1/2 chain model,[8] and the interchain magnetic interactions (zJ) have been treated in the frame of the mean-field approximation[9]

$$\chi_{\text{chain}} = \frac{Ng^2\mu_B{}^2}{kT} \times \frac{0.25 + 0.074975x + 0.075235x^2}{1.0 + 0.9931x + 0.172135x^2 + 0.757825x^3}$$

where

$$x = \frac{|J|}{kT}$$

$$\chi = \frac{\chi_{\text{chain}}}{1 - \frac{2zJ'}{Ng^2\mu_B{}^2}\chi_{\text{chain}}}$$

The obtained best sets of parameters are J = −74.4 cm^{-1}, zJ'/k_B = −1.89 cm^{-1}, and the averaged g factor for the magnetic susceptibility is g_{av} = 2.02 using the data above 30 K to avoid some additional magnetic contribution such as paramagnetic impurity. Complex **1** exhibits a relatively strong intrachain antiferromagnetic interaction between Cu(II) ions via the oxamato bridge. The weak interchain antiferromagnetic interaction is probably mediated by the hydrogen bond between oxamato O atoms through interstitial water molecules. The intrachain antiferromagnetic interaction is comparable to those observed in the oxamato-bridged dinuclear Cu(II) complexes (−J = 4.8–425 cm^{-1}).[10] The coplanar arrangement of two Cu(II) d_{x2-y2} magnetic orbitals through the oxamato bridge is known to lead to the strong antiferromagnetic coupling. Complex **1** has a square pyramidal environment in which the axial position is occupied by one of the oxygen atoms of the oxamato bridge on the neighboring complex, O(2), O(5), and O(8). The neighboring d_{x2-y2} magnetic orbitals along the chain are perpendicular to each other through the oxamato bridge, whose overlap is unfavorable due to magnetic interaction, as described by Kahn.[11] Thus, the J values of **1** are relatively weak as compared with that of the reported complexes with the oxamato bridge.

CONCLUSIONS

The left-handed helical chain of **1**, belonging to space group $P3_2$, was generated by self-assembly of [Cu(L)] and structurally characterized by single-crystal X-ray diffraction study. Coordination of the oxamato moiety to the vacant cite of Cu(II) ions induces the chirality of chain. The oxamato bridge also mediated relatively strong antiferromagnetic interactions between Cu(II) metal ions. Solid-state CD spectra demonstrated the homochirality of crystals obtained in our lab. It is a rare example of homochiral crystallization based on achiral building blocks in the absence of any chiral source.

ASSOCIATED CONTENT

Supporting Information

Crystallographic information file (CIF) for **1**, Curie–Weiss plot, and CD spectrum in saturated aqueous solution of **1**. This material is available free of charge via the Internet at http://pubs.acs.org.

AUTHOR INFORMATION

Corresponding Author

*E-mail: chihiro.kachi@chem.sci.toho-u.ac.jp.

Present Addresses

[⊥]Department of Chemistry, Faculty of Science, Toho University, 2-2-1 Miyama, Funabashi, Chiba 274-8510, Japan.
[#]Research Institute for Science & Technology, Tokyo University of Science, 2641, Yamazaki, Noda, Chiba, Japan.

Notes

The authors declare no competing financial interest.

ACKNOWLEDGMENTS

This work was financially supported by the "High Tech Research Center" Project 2005-2009 and a Grant-in-Aid for Scientific Research from the Ministry of Education, Culture, Sports, Science, and Technology (MEXT), Japan.

REFERENCES

(1) (a) Mason, S. *Chem. Soc. Rev.* **1988**, *17*, 347–359. (b) Avalos, M.; Babiano, R.; Cintas, P.; Jiménez, J. L.; Palacios, J. C.; Barron, L. D. *Chem. Rev.* **1998**, *98* (7), 2391–2404. (c) Jorissen, A.; Cerf, C. *Origins Life Evol. Biosphere* **2002**, *32* (2), 129–142. (d) Weissbuch, I.; Lahav, M. *Chem. Rev.* **2011**, *111* (5), 3236–3267.

(2) (a) Kondepudi, D. K.; Kaufman, R. J.; Singh, N. *Science* **1990**, *250* (4983), 975–976. (b) Kondepudi, D. K.; Bullock, K. L.; Digits, J. A.; Hall, J. K.; Miller, J. M. *J. Am. Chem. Soc.* **1993**, *115* (22), 10211–10216. (c) Kondepudi, D. K.; Bullock, K. L.; Digits, J. A.; Yarborough, P. D. *J. Am. Chem. Soc.* **1995**, *117* (1), 401–404.

(3) Matsuura, T.; Koshima, H. *J. Photochem. Photobiol., C* **2005**, *6* (1), 7–24 and references therein.

(4) (a) Telfer, S. G.; Sato, T.; Kuroda, R. *Angew. Chem., Int. Ed.* **2004**, *43*, 581–584. (b) Telfer, S. G.; Kuroda., R. *Chem.—Eur. J.* **2005**, *11*, 57–68. (c) Khatua, S.; Harada, T.; Kuroda, R.; Bhattacharjee, M. *Chem. Commun.* **2007**, 3927–3929. (d) Yamagishi, A.; Sato, H. *J. Photochem. Photobiol., C* **2007**, *8* (2), 67–84. (e) Amouri, H.; Gruselle, M. *Chirality in transition metal chemistry: molecules, supramolecular assemblies and materials*; Wiley: Chichester, U.K., 2008 and reference cited therein. (f) Telfer, S.; Parker, N.; Harada, T.; Kuroda, R.; Lefebvre, J.; Lenzoff, D. *Inorg. Chem.* **2008**, *47*, 209–218. (g) Crassous, J. *Chem. Soc. Rev.* **2009**, *38* (3), 830–845.

(5) Parsons, S.; Mallah, T.; Winpenny, R.; Wood, P. *Private Communication*, 2004.

(6) Kuroda, R.; Harada, T.; Shindo, Y. *Rev. Sci. Instrum.* **2001**, *72* (10), 3802–3810.

(7) Flack, H. D. *Acta Crystallogr., Sect. A* **1983**, *39*, 876–881.

(8) Estes, W. E.; Gavel, D. P.; Hatfield, W. E.; Hodgson, D. J. *Inorg. Chem.* **1978**, *17* (6), 1415−1421.
(9) For example, see: (a) Myers, B. E.; Berger, L.; Friedberg, S. J. *Appl. Phys.* **1969**, *40*, 1149−1151. (b) O'Connor, C. J. *Prog. Inorg. Chem.* **1982**, *29*, 203−283.
(10) (a) Verdaguer, M.; Kahn, O.; Julve, M.; Gleizes, A. *Nouv. J. Chim.* **1985**, *9* (5), 325−334. (b) Costa, R.; Garcia, A.; Ribas, J.; Mallah, T.; Journaux, Y.; Sletten, J.; Solans, X.; Rodriguez, V. *Inorg. Chem.* **1993**, *32*, 3733−3742. (c) Emori, S.; Todoko, K. *Bull. Chem. Soc. Jpn.* **1993**, *66*, 3513−3515. (d) Aukauloo, A.; Ottenwaelder, X.; Ruiz, R.; Journaux, Y.; Pei, Y.; Rivière, E.; Muñoz, M. C. *Eur. J. Inorg. Chem.* **2000**, *5*, 951−957. (e) Tercero, J.; Diaz, C.; Ribas, J.; Mahia, J.; Maestro, M.; Solans, X. *J. Chem. Soc., Dalton Trans.* **2002**, 2040−2046. (f) Tercero, J.; Diaz, C.; Ribas, J.; Mahía, J.; Maestro, M. A. *Inorg. Chem.* **2002**, *41*, 5373−5381. (g) Ottenwaelder, X.; Cano, J.; Journaux, Y.; Rivière, E.; Brennan, C.; Nierlich, M.; Ruiz-García, R. *Angew. Chem., Int. Ed.* **2004**, *43*, 850−852. (h) Pardo, E.; Bernot, K.; Julve, M.; Lloret, F.; Cano, J.; Ruiz-Garcia, R.; Pasan, J.; Ruiz-Perez, C.; Ottenwaelder, X.; Journaux, Y. *Chem. Commun.* **2004**, 920−921. (i) Pardo, E.; Bernot, K.; Lloret, F.; Julve, M.; Ruiz-García, R.; Pasán, J.; Ruiz-Pérez, C.; Cangussu, D.; Costa, V.; Lescouëzec, R.; Journaux, Y. *Eur. J. Inorg. Chem.* **2007**, 4549−4573. (j) Pardo, E.; Cangussu, D.; Lescouëzec, R.; Journaux, Y.; Pasán, J.; Delgado, F. S.; Ruiz-Pérez, C.; Ruiz-García, R.; Cano, J.; Julve, M.; Lloret, F. *Inorg. Chem.* **2009**, *48*, 4661−4673.
(11) Kahn, O. *Molecular magnetism*; VCH: New York, 1993.